INL/CON-07-12672
PREPRINT

Design and Testing of a Unique Active Compton-Suppressed LaBr$_3$(Ce) Detector System for Improved Sensitivity Assays of TRU in Remote-Handled TRU Wastes

2007 Nuclear Science Symposium

John K. Hartwell
Michael M. McIlwain
Jonathan A. Kulisek

October 2007

The INL is a
U.S. Department of Energy
National Laboratory
operated by
Battelle Energy Alliance

Idaho National Laboratory

Design And Testing Of A Unique Active Compton-Suppressed LaBr$_3$(Ce) Detector System For Improved Sensitivity Assays Of TRU In Remote-Handled TRU Wastes

John K. Hartwell, *Member, IEEE*, Michael M. McIlwain, Jonathan A. Kulisek

Abstract– **The US Department of Energy's transuranic (TRU) waste inventory includes about 4,500 m^3 of remote-handled TRU (RH-TRU) wastes composed of a variety of containerized waste forms having a contact surface dose rate that exceeds 2 mSv/hr (200 mrem/hr) containing waste materials with a total TRU concentration greater than 3700 Bq/g (100 nCi/g). As part of a research project to investigate the use of active Compton-suppressed room-temperature gamma-ray detectors for direct non-destructive quantification of the TRU content of these RH-TRU wastes, we have designed and purchased a unique detector system using a LaBr$_3$(Ce) primary detector and a NaI(Tl) suppression mantle.**

The LaBr$_3$(Ce) primary detector is a cylindrical unit ~25 mm in diameter by 76 mm long viewed by a 38 mm diameter photomultiplier. The NaI(Tl) suppression mantle (secondary detector) is 175 mm by 175 mm with a center well that accommodates the primary detector. An important feature of this arrangement is the lack of any "can" between the primary and secondary detectors. These primary and secondary detectors are optically isolated by a thin layer (.003") of aluminized Kapton. This arrangement virtually eliminates the "dead" material between the primary and secondary detectors, a feature that preliminary modeling indicated would substantially improve the Compton suppression capability of this device.

This paper presents both the expected performance of this unit determined from modeling with MCNPX, and the performance measured in our laboratory with radioactive sources.

I. INTRODUCTION

T HE US Department of Energy's Remote-Handled Transuranic (RH-TRU) waste inventory presents a unique characterization challenge to gamma-ray spectrometric techniques. The Compton scattering continuum generated by the interaction of higher energy gamma-rays from the nuclides contributing the >2 mSv/hr surface dose rate in the waste matrix and in the detector obscures the lower energy, low-yield gamma-ray peaks from the TRU decay. The unique

detector tested in this work was designed and procured to improve the detector peak-to-Compton ratio to facilitate the use of room temperature detectors for RH-TRU characterization.

II. DETECTOR DESIGN AND MODELING

The detector system is depicted in the sketch of Figure 1. The LaBr$_3$(Ce) primary detector is a cylindrical unit ~25 mm in diameter by 76 mm long viewed by a 38 mm diameter photomultiplier (PMT.) The NaI(Tl) suppression mantle (secondary detector) is 175 mm by 175 mm with a center well that accommodates the primary detector. An important feature of this arrangement is the lack of any "can" between the primary and secondary detectors. The primary and secondary detectors are optically isolated by a thin layer (.003") of aluminized Kapton, but the hermetic seal and thus the aluminum can surrounds the outer boundary of the detector system envelope. The hermetic seal at the primary detector PMT is at the PMT wall. This arrangement virtually eliminates the "dead" material between the primary and secondary detectors, a feature that preliminary modeling indicated would substantially improve the Compton suppression capability of this device [1].

During the detector design, the expected performance was modeled using MCNPX Version 2.5.0 [2] using the anticoincidence pulse-height tally option. The Gaussian energy broadening (GEB)
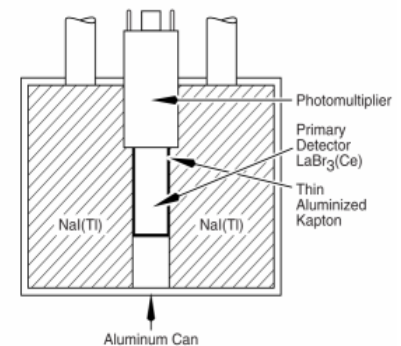

Fig 1 Detector configuration

feature of MCNPX was also used to model the resolution of the LaBr$_3$(Ce) detector. The GEB feature estimates the FWHM of a unit as:

$$FWHM = a + b\sqrt{E + cE^2}$$

. We determined the a, b, and c parameters for this relation from a curve fit to resolution measurements that we performed at eight different energies

ranging from 238 keV to 2614 keV on a Ø38 mm by 38 mm long LaBr$_3$(Ce) detector in our laboratory. The resolution at 662 keV was measured to be ~ 2.8 %, consistent with previous work [3]. The secondary detector cutoff energy (the minimum amount of energy that must be deposited in the secondary detector in order to trigger rejection) was chosen at 10 keV.

The figure of merit primarily used to measure the efficacy of the modelled suppression performance is the suppression factor, defined as:

$$\text{Suppression Factor} = \frac{P(\Delta E)NS}{P(\Delta E)S}$$

Here, P(ΔE)NS is the probability of events in the energy range ΔE without using suppression, and P(ΔE)S is the probability of events in energy range ΔE using suppression. The suppression factors were computed for the [137]Cs Compton region from 358 to 382 keV.

The MCNPX calculations predicted that the expected Compton suppression performance was sensitive to the position of the primary detector within the NaI(Tl) well. Our initial design [4] placed the LaBr$_3$(Ce) primary at the back of the well in order to simplify the mounting of the primary PMT; however, the design was changed to that of Figure 1 (with a centered primary detector) after the modeling results suggested that such a rearrangement could dramatically improve the Compton suppression factor at the Compton region of [137]Cs (358 to 382 keV) from about 23 to about 60. The model results (suppressed and unsuppressed) for a ^{137}Cs source located 20 cm from the face of a 5 mm diameter circular collimator (5.1 cm thick) coaxial to the primary detector centerline are presented in Figure 2. Due to limitations in the MCNPX model the contribution to these spectra from the intrinsic [138]La activity within the detector [5] is not modeled.

Fig. 3 MCNPX model results for Compton suppression performance as a function of spectral energy. The incident photons are 662 keV gamma rays. The suppression will be near its maximum for the 413.7 keV line from [239]Pu.

III. EXPERIMENTAL MEASUREMENTS

A. Measurement Technique

A scintillation detector fabricated to replicate the features of the unit modeled in MCNPX was procured, and is under preliminary testing in our laboratory. The LaBr$_3$(Ce) primary detector is viewed by a Photonis XP2060/B02 PMT, while the NaI(Tl) mantle is equipped with four ETI 9266 PMTs. A manufacturer-supplied preamplifier was used on the output of the LaBr$_3$(Ce) primary detector. Fig 4 shows two different views of this unit.
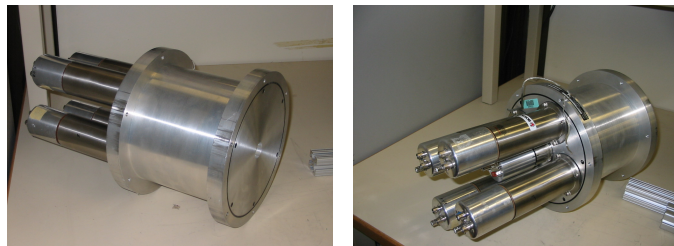
Fig 4 Photos of the LaBr$_3$(Ce)/NaI(Tl) active suppression detector assembly from two different views. In the rear view, the centered, recessed PMT that views the integral LaBr$_3$(Ce) detector, and it's plug-on preamplifier are clearly visible.

The procured unit differed slightly from the modeled unit in the configuration of the NaI(Tl) suppression guard. The modeled unit was one monolithic NaI(Tl) crystal; however, the purchased unit consisted of four optically-isolated "pie wedge"shaped crystals each viewed by its own PMT. This modification increased the light collection efficiency of each PMT, and decreased the detector cost; however, it introduced a thin dead layer of optical isolation wrap (similar to Teflon) at the interface of each wedge-shaped crystal.

The resolution performance of the LaBr$_3$(Ce) primary detector and the NaI(Tl) detectors were tested. At 662 keV the photopeak resolution of the LaBr$_3$(Ce) primary detector was measured as 3.0%±0.2% FWHM in agreement with the
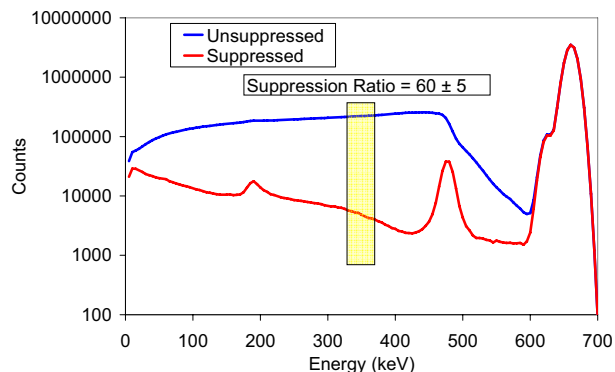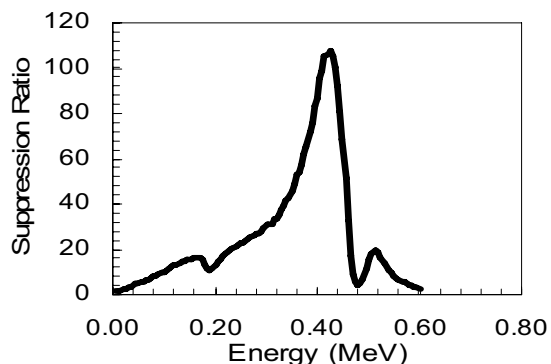

Fig 2 Results of the MCNPX model for suppression performance of the detector for a collimated ^{137}Cs source. The highlighted region is the 358 to 382 keV Compton region. The pronounced shoulder on the low energy side of the ^{137}Cs photopeak is from escape of the La X-rays.

manufacturer's specification. The NaI(Tl) PMTs were adjusted for gain matching, and the 662 keV photopeak resolution of each detector tested separately and as a unit. The individual resolutions varied from 5.8% to 6.5% FWHM and the measured resolution of the overall unit with outputs connected in series (ORed) was 6.7% FWHM.

Also, since contamination of lanthanum-based scintillators with radioactive ^{227}Ac is a know problem, we checked the background in the associated energy region between 1600 and 2800 keV, and we did find peaks from the alpha-particle emissions from ^{227}Ac plus its daughters. However, the total alpha peak count rate was only 0.0166 ± 0.0003 counts/s/cm^3 of detector volume, a value lower than we have measured on other lanthanum-based scintillators [5].

The LaBr$_3$(Ce) primary detector was biased at +720 V and the output of the preamplifier provided to the input of a shaping amplifier (TC244). The amplifier provided a gain of about X5 and was set for a triangular shaped output pulse with a peaking time of 0.5 µs (shaping time 0.25 µs). The shaped output pulse was routed to the input of either a "Pocket MCA" (Amptek 8000A), or an Ortec "TRUMP" card. The MCAs were set for a conversion gain of 2048 channels with a full scale +10 V input. These settings placed the 662 keV peak of ^{137}Cs in the upper half of the spectrum.

The four NaI(Tl) PMTs were equipped with standard tube bases (Bicron P-14s) with a +1250V bias. Two electronics configurations were tested for the Compton suppression system. In both configurations, the daisy-chained (ORed) output of the tube bases was input to a Timing Filter Amplifier (TFA). The TFA provided a modest gain and some signal conditioning while maintaining a reasonably fast pulse. The TFA output pulse was routed to a Constant Fraction Discriminator (CFD) operating in the leading edge mode. The CFD threshold was carefully set to a level very slightly into the noise threshold. While this generates some spurious vetos, it ensured cancellation down to and below a 10 keV signal level. (This was confirmed by testing.) In one electronic configuration (termed a "direct shield veto" mode) the positive square wave output of the CFD was stretched to 2 µs in width using a Gate and Delay Generator and when suppression was desired this pulse was provided to the gate input of the MCA operating in anticoincidence mode. Note that this mode exerts a veto regardless of the presence or absence of an associated primary detector event. An alternative electronic configuration was also tested that required a coincidence between a shield event and a primary detector event before a veto was issued. This configuration, termed a "positive logic veto" system has been used successfully at our laboratory and by others [6]. No significant differences in Compton suppression performance were noted between the direct shield veto and the positive logic veto systems; however, at elevated shield count rates the full shield veto technique resulted in higher losses from full energy peak of the primary detector spectrum than did the positive logic

veto configuration, so the latter configuration was used for the work reported here.

A shield, collimation, and optical rail system were configured to facilitate laboratory testing of this unit. The detector assembly was positioned behind a lead and tungsten shadow shield (5-cm thick) that protected the detector from direct test source gamma rays. A 5-cm thick tungsten collimator block with inserts to provide circular apertures of 14, 10, 5, and 2 mm diameters was configured using the optical rail system to allow a test source (also positioned on the rail) to irradiate the center of the LaBr$_3$(Ce) primary detector face without direct irradiation of the secondary NaI(Tl) guard detector. This setup emulates the MCNPX-modeled configuration. Figures 5 and 6 are photographs of this configuration.

Fig. 5 A photograph of the optical rail system configured for testing of the Compton suppression detector assembly (at the far left.) The fixture attached to the rail at the far right of the photo is the aluminum source holder.
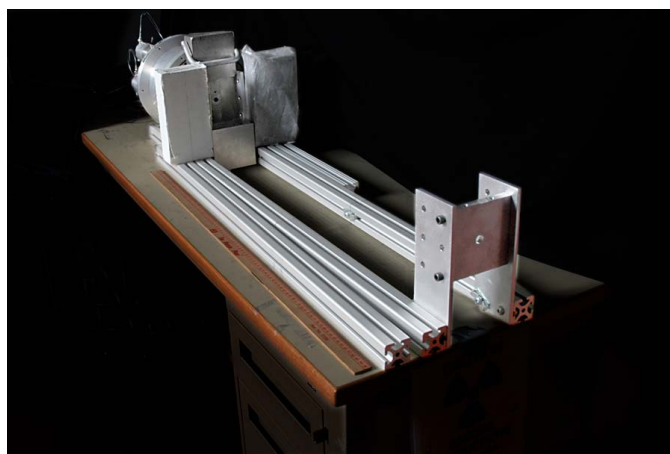

Fig. 6 A view of the test apparatus from the source end. The circular collimator aperture in the centered tungsten shielding block is visible in this view. Point sources were aligned with the collimator aperture by securing them to the aluminum plate visible at the near end of the optical rail, and centering the source active region in the hole of the plate. The source-to-detector distance was set by adjusting the source holder position on the optical rail.

During our test measurements, the entire test assembly – optical rail, source, detector, and detector assembly, collimator

and shadow shield – were housed in a shield that surrounded the entire assembly with 10 cm of lead shielding (lined with tin and copper grading.) This arrangement significantly decreased the shield detector counting rate relative to bench top measurements.

B. Experimental results

The measured Compton suppression performance of this unit has not approached the modeled expectations. Figure 7 presents the best suppression performance measured under the modeled conditions of a 5-mm diameter circular collimator aperture and a ^{137}Cs point source 20 cm from the collimator entrance. The measured suppression factor of 12.1 ± 0.7 is much poorer that the model prediction of 60 ± 5 (see Fig. 2.)
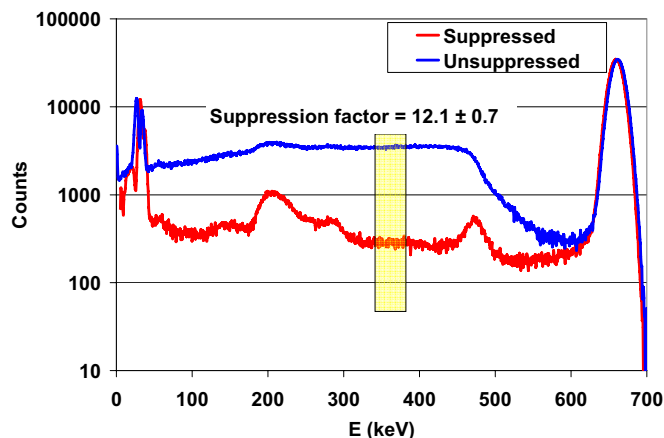

Fig. 7 Measured suppression performance for the LaBr3/NaI detector in the modeled configuration. A 137Cs point source was located 20 cm from the entrance of 5 mm diameter collimator. The highlighted region is the Compton region from 358 keV to 382 keV.

In these measurements the peak-to-Compton ratio improved from 9.9:1 to 119:1 with the suppression system active. The peak-to-total ratio without suppression was 0.33 and improved to 0.69 with the suppression system active.

We have compared the measured suppression factors as a function of energy with those predicted by the MCNPX model (see Fig. 3.) To facilitate this comparison we scaled the MCNPX model predictions (that had a maximum predicted suppression factor of 118 to match the measured maximum suppression factor of 16. This comparison is presented in Figure 8. While some of the features are similar in their energy profile, the model predicts a much more strongly peaked suppression performance than was measured.

The highly peaked nature of the model results is highlighted in Fig. 9. Fig 9 presents the energy dependent ratio of the modeled suppression ratio to the measured suppression ratio. The average discrepancy between modeled and measured suppression factor is a ratio of about 3; however this difference is strongly peaked in the 350 to 450 keV region. For this energy deposition in the primary detector the scattered photons leave the primary detector at angles between about 90 and 140 degrees, thus irradiating primarily the forward half of the secondary detector.
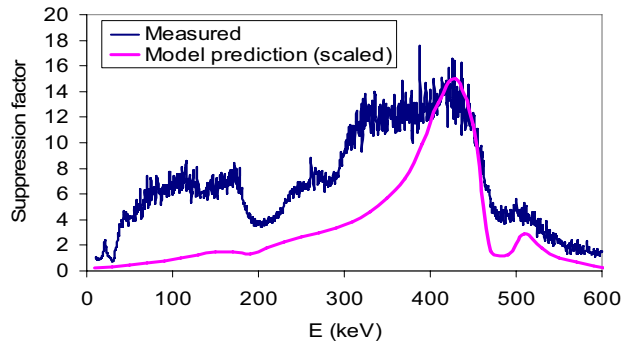

Fig. 8 Comparison of the energy dependence of the measured and modeled suppression factor performance of the detector assembly. The MCNPX-modeled suppression factors have been scaled by a factor of 0.135 in order to match the maximum of the measured values.
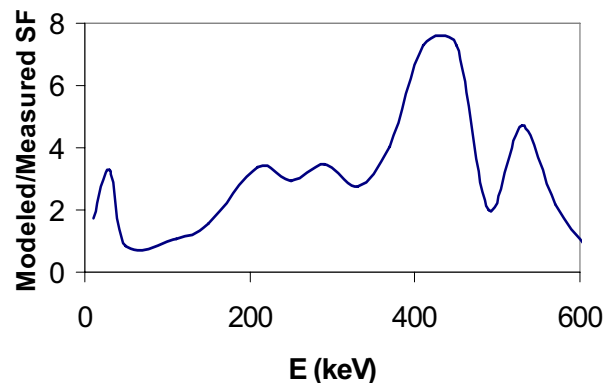

Fig. 9 A plot of the modeled suppression factor divided by the measured suppression factor as a function of the energy depeosited in the primary LaBr$_3$(Ce) detector.

C. Transuranic spectra

To aid in our assessment of the efficacy of this detector unit for measurement of transuranic isotopes, we acquired a spectrum on an aged sample of low-burnup ("weapons grade") plutonium. The sample was small (14 mg) and thus was counted close to the collimator aperture; however, the measured spectral count rates were mathematically adjusted to estimate the spectrum expected for a one gram source of aged low-burnup plutonium located 20 cm in front of a 5-mm diameter collimator. This spectrum is presented in Fig 10. When compared to published [7] spectra taken with NaI(Tl) detectors, the improved resolution of the LaBr$_3$(Ce) primary detector is obvious. In NaI(Tl) spectra the triplet complex

between 300 and 450 keV is completely unresolved, and the 125-129 keV peak is not resolved from the X-ray complex below it.
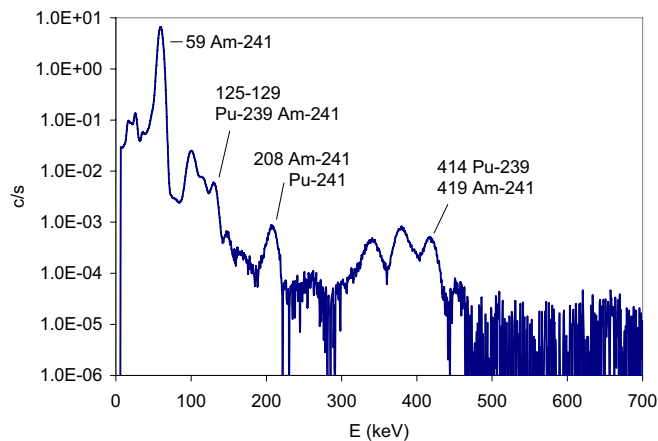

Fig. 10 Suppressed spectrum for 1 gram of aged weapons grade plutonium 20 cm from a 5 mm collimator entrance. All of the prominent peaks are from either ^{241}Am or ^{239}Pu. Some of the important assay lines are identified with the line energy in keV and the most strongly contributing isotopes.

IV. DISCUSSION

The reason for the discrepancy between the modeled and measured Compton suppression performance of this detector is not understood. The model has been carefully reviewed and with the minor exception of the segmentation of the NaI(Tl) secondary detector, the model reproduces the detector dimensions provided by the manufacturer. The discrepancy is particularly puzzling since prior MCNPX models of suppression behavior for a more conventional active anti-Compton-guarded system showed reasonable agreement with the laboratory measurements [1]. Similarly, we are confident the veto system is working properly.

The measured suppression performance of this detector, assuming a simple detection model of sensitivity being inversely proportional to the square root of the background, should improve the detection sensitivity for the 129 keV and 413 keV lines of ^{239}Pu by factors of about 2.6 and 3.9 respectively relative to a similar unsuppressed detector. If the modeled performance had been realized, these respective sensitivity improvement factors would have been about 5 and 10 respectively.

We will continue to investigate the difference between modeled and measured active suppression behavior. However, the combination of room-temperature operation, high detection sensitivity, and sufficient resolution to separate particularly the ^{239}Pu assay line at 414 keV from significant interferences suggest that this unit may have applications in other nuclear material measurement applications less demanding than the direct assay of remote-handled TRU wastes.

V. REFERENCES

[1] W. Scates, J. K. Hartwell, R. Aryaeinejad, M.E. McIlwain, "Optimization studies of a Compton suppression spectrometer using experimentally validated Monte Carlo simulations," *Nucl. Inst. and Meth.* A 556, pp.498-504, 2006.

[2] D. B. Pelowitz, ed., *MCNPX User's Manual Version 2.5.*0, Los Alamos National Laboratory, April 2005.

[3] E. V. D van Loef, P. Dorenbos, C. W. E. van Ejik, K. Kramer, and H. U. Gudel, "Scintillation properties of LaBr$_3$:Ce^{3+} crystals: fast, efficient and high-energy-resolution scintillators," *Nucl. Inst. and Meth.*, A486, pp. 254-258, 2002.

[4] J. A. Kulisek,, J. K. Hartwell, M. E. McIlwain, and R. P. Gardner, "Design and Preliminary Monte Carlo Calculations of an Active Compton Suppressed LaBr$_3$(Ce) Detector System for TRU Assay in Remote-Handled Wastes," *Nucl. Inst. and Meth.* A580, issue 1, p. 226-229, 2007.

[5] J. K. Hartwell and R. J. Gehrke, "Observations on the background spectra of four LaCl$_3$(Ce) scintillation detectors," *Appl. Radiat. Isot.*, 63, p. 223-228, 2005.

[6] C. S. Lee, *et al*, "Characteristics of a Transverse-Type Compton-Suppressed Gamma-ray Detector," *Journal of the Korean Physical Society*, 40, pp 807-811, 2002.

[7] H. A. Smith and M. Lucas, "Gamma-ray Detectors," in *Passive Nondestructive Assay of Nuclear Materials*, D. Reilly, N. Esslin, H. Smith, and S. Kreiner, Eds.,Los Alamos National Laboratory Technical Report LA-UR-90-732 , March, 1991.